

Surface Potential Imaging For Magnetoresistive Head Development[†]

John Moreland and S. E. Russek
Electromagnetic Technology Division, National Institute of Standards and Technology
Boulder, Colorado 80303, USA

P. F. Hopkins
Quantum Peripherals Colorado, Inc.
Louisville, Colorado 80027, USA

Abstract. - We demonstrate the first applications of scanning surface potential microscopy to magnetoresistive (MR) thin-film devices. Images are presented on active devices showing 2D maps of the surface potential of energized MR read-head stripes taken from the production line at the puck level. We have found that surface potential line scans (voltage vs. distance) along MR spin valve stripes show slight deviations from linearity, possibly due to nonuniform film magnetization along the length of the stripe.

I. INTRODUCTION

In this paper we present surface potential images of thin-film magnetoresistive (MR) devices measured by atomic force microscopy (AFM). In this method, surface potential is determined by measuring the motion of a conductive AFM cantilever due to the capacitive forces between the tip and the sample. This technique is useful for measuring surface potential shifts generated by current flowing through a device. It is also sensitive to spatial variations of work functions, contact potentials, and trapped charges. We give a brief argument for choosing this method over others and demonstrate its usefulness for imaging variations of the MR coefficient as a function of position with 50 nm resolution. We are motivated by the fact that the local MR coefficient of a thin-film multilayer depends on the nanometer-scale details of domain pinning and magnetic biasing. These effects are not well understood especially for patterned devices with micrometer and submicrometer dimensions.

One of the first variations to scanning tunneling microscopy (STM) was scanning tunneling potentiometry (STP) [1,2]. STP has been demonstrated to have a voltage sensitivity at the 100 nV level using a tunneling current nulling scheme to determine local surface potential. STP works well on conductive samples where a practical tunneling contact can be maintained during scanning. The atomic force microscope (AFM) has also been adapted for scanning potentiometry [3]. The advantage of AFM is that part of the sample being scanned can be insulating. This advantage is crucial for potentiometry of submicrometer devices where it would be difficult to position a STM tip on the sample without crashing the tip on adjacent insulating regions.

What mode of operation is the best for AFM potentiometry? Requirements to be considered for industrial applications include nanometer spatial resolution, prospects for submillivolt resolution,

Manuscript received April 10, 1997.

Moreland, 303-497-3641, fax 303-497-7676, moreland@boulder.nist.gov; S. E. Russek, 303-497-5097, fax 303-497-5316, russek@boulder.nist.gov; P. F. Hopkins, 303-604-5401.

[†]Contribution of the National Institute of Standards and Technology, not subject to copyright.

practical scan times, calibration, simplicity of operation, ambient operation in air, and operator expertise. AFM potentiometry can be divided into two general categories - contact or noncontact. By definition, contact mode means that the tip and sample surfaces are in electrical contact, whereas in noncontact mode it is the long range electric forces between the tip and the sample surface that are used to deduce local voltage shifts. Contact-mode potentiometry has the advantage of high spatial and voltage resolution if measurable electrical contact can be maintained while scanning. This can be difficult (as discussed below) due to surface contamination between the tip and the sample. Electrical contact is not a problem in noncontact mode. However, since electric forces between the tip and the sample are long range, spatial resolution is limited.

An AFM cantilever is designed to limit the contact force to less than 10 nN so that it is nondestructive. This is a source of difficulty when performing contact-mode AFM potentiometry since both the cantilever tip and sample may have a surface contamination layer. During STP, the rigid STM tip pushes any fluid layers away and breaks through any thin oxide in order to establish tunneling contact to the sample. Movement of an AFM cantilever tip, on the other hand, can be dominated by water surface tension between the tip and the sample in addition to the presence of surface oxides[4]. Meepagala, *et al.* showed that a water layer prevents electrical contact between the presumably clean surfaces of a Au-coated tip and a Au sample in air [5]. Even if fluid and oxide effects could be minimized, the area of the contact is small for low cantilever forces. In the Sharvin limit, where the mean free path, l , is much larger than the radius of the contact, a , the resistance is given by $R_{\text{contact}} = (4/3) \pi \rho l / a^2$ [6]. For typical metals, $\rho l = 5 \cdot 10^{-12} \Omega \cdot \text{cm}^2$, so that for an atomic level contact with $a = 0.3 \text{ nm}$, R_{contact} is about 20 k Ω which is marginal for contact potentiometry. In reality, low-force AFM contacts in air are nonideal and have much higher resistances above 1 G Ω making direct-contact voltage measurements impractical. Unfortunately, we have found that the tip-sample forces have to be very high (greater than 1 μN) to make low-resistance electrical contact. This force would be damaging to both the tip and sample, and cause wear in a scanning mode. In addition, large forces cause the tip to slide along the surface so that the precise location of the electrical contact on the sample is unknown relative to the piezo-positioning system.

II. EXPERIMENTAL

The details of the modifications to an AFM required for noncontact surface potential imaging are discussed by Yokoyama and Inoue [7]. The surface potential on the sample is measured by applying a voltage $V = V_{\text{dc}} + V_{\text{ac}} \sin(\omega t)$ between the AFM tip and the sample. The capacitive force between the tip and the sample is

$$F = \frac{\partial}{\partial z} \left(\frac{1}{2} CV^2 \right). \quad (1)$$

Making the approximation that the tip can be modeled as a thin capacitor plate of radius r at a distance z above the sample, with a capacitance of $C = \epsilon\pi r^2/z$, the capacitive force component at ω is

$$F_{\omega} = \epsilon\pi V_{dc} V_{ac} \left(\frac{r}{z} \right)^2 \sin(\omega t). \quad (2)$$

Equation (2) shows that F_{ω} can be minimized by adjusting the dc voltage applied to the tip so that $V_{dc} \rightarrow 0$. This is done with a feedback loop at each point along the surface during imaging. As is the case for magnetic force microscopy, the spatial resolution of the surface potential is limited to about 50 nm by the radius of curvature of the tip and the scan height which are both about 20 nm.

A minimum F_{ω} of 1 pN is typical of our AFM which has a narrow-bandwidth detection scheme based on phase-locked loop detection of the cantilever motion near resonance. In this case, with the estimate that $z \approx r$ and using $V_{ac} = 5$ V, we estimate a local surface potential sensitivity of 1 mV. Experimentally, the noise level is in the range from 1 to 10 mV depending on the tip.

The AFM tip must be coated with a thin conductive layer that is tough and does not easily corrode in air. We coated commercially available Si micromachined cantilevers (resonant frequencies of 70 to 89 kHz and spring constants of 1 to 5 N/m) with 20 nm of Cr evaporated from a Cr-coated W rod at a deposition rate of 0.3 nm/s in a background vacuum of 1.3×10^{-4} Pa (10^{-6} Torr).

Measurements were made by interleaving line scans with the AFM in different modes. First, the surface topography was measured followed by a retrace in surface potential mode along the same line, but with the tip lifted at $z = 100$ nm above the sample. In all cases $V_{ac} = 5$ V.

III. RESULTS

Noncontact AFM scanning potentiometers are sensitive to many sources of surface potential. This is illustrated in Fig. 1, which shows the surface topography image (Fig. 1a), the surface potential image (Fig. 1b), and the surface potential line scan (Fig. 1c) of a MR read-head sensor biased at $I = 10$ mA. The device was one of many on the surface of a puck taken from the production line before dicing and polishing. There is a 0.2 V potential increase from left to right along the MR stripe. Other contributions to the potential, however, which correlate with surface topography; these include potential shifts near micrometer-sized particles at the edges of the strip as well as the shallow trench crossing the stripe. These "excess" surface potentials may come from different charged surface layers on the MR stripe, the current leads, or the trench, which are left over from fabrication. Alternatively, they may come from the contact potential between the current leads and the MR stripe.

As a first step toward separating the different sources of surface potential in scanning potentiometry images, we have performed experiments on spin valve stripes [8]. The spin valve sample is designed for digital applications and should ideally have only two resistance states.

Image subtraction is helpful when imaging small magnetoresistive shifts of MR devices. The voltage drop along a MR stripe is expected to be linear along the stripe as a function of distance. As an

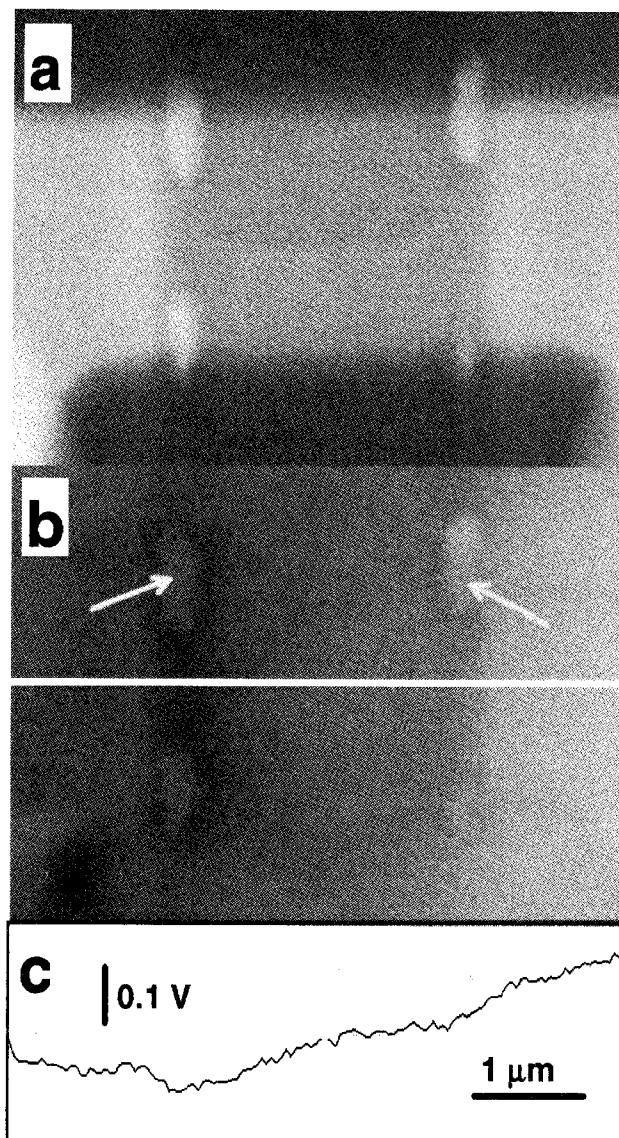


Fig. 1. Images of an MR device developed for a read head showing: (a) surface topography; (b) surface potential; and (c) a line scan of surface potential along the axis of the device as shown in Fig. 1b. Arrows show charged particles.

external magnetic field is applied to the device we expect the surface potential line scan (voltage vs. distance) to remain uniformly linear but with different slope. However, slight deviations from linearity could in principle occur due to the formation of extended regions of the device with a different sheet resistance relative to neighboring regions. Local resistance variations may be caused by domain pinning or magnetic field self biasing from the current flowing in the device. Depending on the MR coefficient for the magnetic layers, these small deviations from linearity can be less than 1% shifts in the local slope of the surface potential line scan and thus difficult to measure. Alternatively, the difference between surface potential line scans taken at different applied fields can be measured point-by-point with the stripe at a fixed current bias. This makes it easier to visualize small changes in the sheet resistance of the stripe. The subtraction process additionally removes common mode artifacts, particularly static surface potentials stemming from surface charging or contact potentials, which presumably do not change with changes in the applied field.

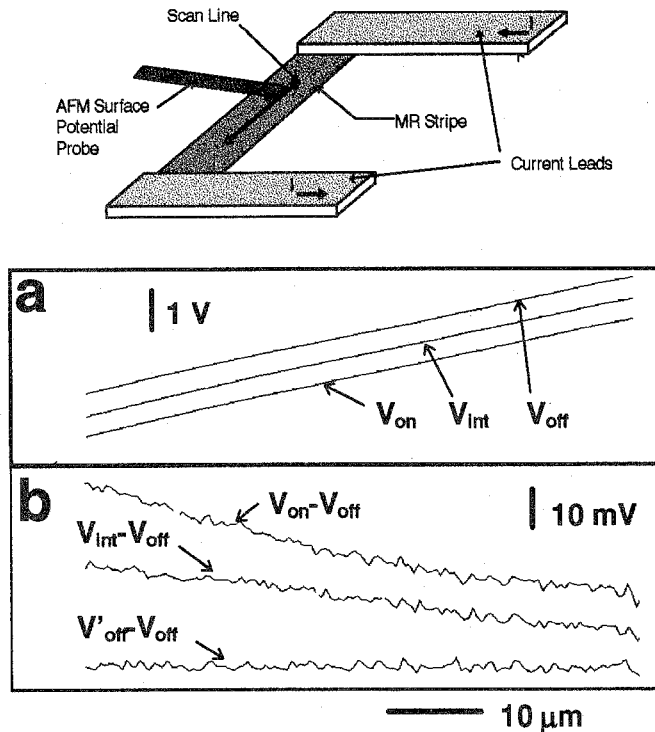


Fig. 2. Surface potential line scans of a GMR spin-valve stripe showing: (a) voltage vs. distance; and (b) subtracted voltage curves (relative to V_{off}) versus distance for different stripe resistance states at different applied fields. The orientation of the AFM tip relative to the stripe is shown at top.

Figure 2 shows the surface potential measurements of a sputter-deposited spin-valve stripe biased at 30 mA. The line scan was limited to half of the stripe due to the scan limit on the piezo-scanner. Each line scan is an average of 16 separate line scans under the same applied magnetic field conditions. The field was adjusted by moving a magnet close to the stripe at various distances and flipping the magnet over to reverse field direction. The overall stripe resistance was monitored during this process. Data taken at stripe resistances of $R = 310, 300,$ and 293Ω , corresponding to surface potential line scans labeled as $V_{on}, V_{int},$ and V_{off} , are shown in Fig. 2a. The magnitude and direction of the field were not well defined during this process. However, the MR hysteresis loop was measured subsequently in a calibrated

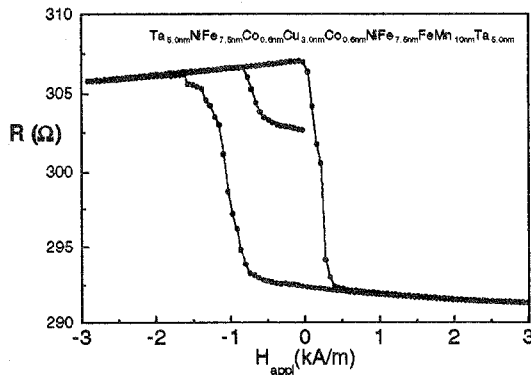


Fig. 3. MR hysteresis loop for the digital spin valve stripe. The device exhibited several intermediate resistance states indicating that complicated domain structures along the length of the device are possible depending on its field history.

electromagnet (see Fig. 3). It is difficult to see any shifts in the surface potential line scans of Fig. 2a; rather we must refer to the subtracted curves in Fig. 2b. The $V'_{off} - V_{off}$ curve is the difference between two curves taken at roughly the same point on the MR hysteresis curve. This provides a check on the noise of the averaging and subtraction processes. Careful observation of the line scans in Fig. 2a shows tiny features due to static contributions in the surface potential which do not show up in the subtracted curves. Also, we see clearly that the $V_{off} - V_{on}$ curve is not linear. We would expect a linear curve for the stripe in different but uniform sheet resistance states.

V. DISCUSSION

Given the uncertainties regarding the direction and magnitude of the applied field for the existing configuration of our AFM scanning system, it is difficult to make quantitative correspondence between the hysteresis curves in Fig. 3 and the surface potential results shown in Fig. 2. Rather we point out the utility of the technique to measure small changes in the local sheet resistance of thin-film stripes by measuring the local slope of the voltage difference line scans as illustrated in Fig. 2b. The hysteresis curve is evidence for domain formation and intermediate MR states in this sample. In addition, the surface potential data support our picture of extended regions of nonuniform magnetoresistance spanning sections of the stripe.

Voltage noise from the cantilever control electronics and the thermal noise of the cantilever itself limit the sensitivity of the potential measurement with the instrument described above. For statistically significant surface potential measurements at submicrometer dimensions, the voltage signal-to-noise ratio (SNR) needs to be improved by about a factor of 10. The force noise of the current instrument is about $1 \text{ pN}/\sqrt{\text{Hz}}$. Improvements in SNR can be obtained by operating in a vacuum to eliminate viscous damping of cantilever excitations. The mechanical Q of the cantilever should increase by more than a factor of 100 in vacuum [9], and since $\text{SNR} \propto \sqrt{Q}$, this should be sufficient for the required voltage sensitivity improvement of our current instrument configuration. Improved voltage sensitivity combined with the 50 nm spatial resolution of the instrument will open up many opportunities for study of small, patterned thin-film conductors and devices. Another extension of the technique includes high frequency operation using the cantilever as an electromechanical mixer based on the nonlinear capacitive force. This mode has been demonstrated by several authors on semiconductor devices [10,11] but has yet to be applied to magnetic thin-film devices.

REFERENCES

- [1] P. Murali and D. W. Pohl, *Appl. Phys. Lett.* **48**, 514 (1986).
- [2] J. R. Kirtley, S. Washburn, and M. J. Bradey, *Phys. Rev. Lett.* **60**, 414 (1988).
- [3] Y. Martin, D. W. Abraham, H. K. Wickramasinghe, *Appl. Phys. Lett.* **52**, 1103 (1988).
- [4] H. G. Hansma, J. Vesenka, C. Siegerist, G. Kelderman, H. Morrett, R. L. Sinsheimer, V. Elings, C. Bustamante, and P. K. Hansma, *Science* **256**, 1180 (1992).
- [5] S.C. Meepagala, F. Real, and C. B. Reyes, *J. Vac. Sci. Technol. B* **9**, 1340 (1991).
- [6] V. Sharvin, *Sov. Phys. JETP* **21**, 655 (1965).
- [7] H. Yokoyama and T. Inoue, *Thin Solid Films* **242**, 33 (1994).
- [8] S. E. Russek, J. O. Oti, Young K. Kim, and R. W. Cross, "Performance Optimization of Submicrometer Spin Valves for Digital Applications," these proceedings.
- [9] T. R. Albrecht, *J. Appl. Phys.* **62**, 668 (1991).
- [10] A. S. Hou, F. Ho, and D. M. Bloom, *Electron. Lett.* **28**, 2302 (1992).
- [11] C. Bohm, C. Roths, and E. Kubalek, *Microelectronic Engineering*, **24**, 91 (1994).